25th ABCM International Congress of Mechanical Engineering
October 20-25, 2019, Uberlândia, MG, Brazil

COB-2019-0735
NUMERICAL HEAT ABSORPTION EFFICIENCY COMPARISON IN THE APPLICATION OF PHASE CHANGE MATERIALS (PCM) ON A MASONRY WALL

Ernandes José Gonçalves do Nascimento
Marcelo José Santos de Lemos
Instituto Tecnológico de Aeronáutica, São José dos Campos - SP, Brasil
ernandesn549@gmail.com
delemos@ita.br

Abstract. *Energy saving technologies are among the highest demand products all around the globe. As many man-made devices are often being improved in order to have electricity as main power source, the cost of this type of energy tends to grow as years go on (for many countries fossil fuels will have to be removed from being a primarily mean of powering vehicles in the next few decades). Thus, this state shows solid signs that saving power appliances will eventually become more cost effective, surpass the expense state and become a low risk investment. With this global scenario background, this work aims to numerically investigate the heat absorption capacity of different phase change materials (PCM) when displaced in standard configuration inside an average thickness masonry wall. The main objective is to map the thermal behavior of a PCM plate vertically positioned along the concrete-brick structure by plotting average volume fraction and average temperature versus time as well as visually investigate the phase change progression in a small cross sectional area. The numerical simulations will be carried on using Star-CCM+ (Siemens PLM Software) code and a simple mesh independency study will be developed in order to ensure the numerical results.*

Keywords: Phase Change Materials, Thermal Insulation, Masonry Wall, Phase Change Simulation, Energy Saving

1. INTRODUCTION

Thermal storage technologies are useful to balance temperature variation amplitude caused by sunlight intermittence. PCMs are usually known for embracing a melting temperature purposely ranged between 19 to 28 ℃ (organic materials) and 25 to 35 ℃ (inorganic materials), as formerly described by Yaping, C. et al., (2015). As soon as this value is reached all the heat surpassing the plate will be direct driven to supply the latent heat of fusion, consequently holding a rise in temperature that would normally occur in case of a standard wall. Further on, as daylight evades and night time arises, all the stored energy will be gradually released to both sides of the wall, which may be particularly useful to keep room thermal comfort in desert regions with a high daily thermal amplitude. However, as this study is being conducted in a thermal research laboratory placed in a tropical region, special emphasis will be given to the use of thermal insulation combined with PCM. As formerly described by Panayiotou, G. P. et al., (2016), a PCM combined with thermal insulation embraces better thermal performance as a mean of maintaining room temperature as solar radiation strikes walls and roof. Therefore, this study will only investigate the use of different PCMs combined with insulation material. By varying the properties and the quantity of PCM layers along the concrete-brick structure it is possible to analyze which configuration is capable of keeping the internal room temperature with the smaller possible variation. As a consequence to this, a lower capacity cooling/heating system will be enough to keep the dwelling interior at a comfortable temperature during all day long, thus providing electricity savings. A recent paper (Panayiotou et al., 2016) well discusses the application of PCMs specifically in the Mediterranean region. This work greatly promotes a complete estimative of the power saved with the application of PCMs in the envelope of a typical dwelling but it also compares its use with the standard insulation materials, which makes it possible to calculate important financial parameters as the investment payback. Panayiotou et al., (2016) then concludes that the use of only PCM will imply in a payback of fourteen and a half years, which can be reduced to seven and a half years just by adding a layer of thermal insulation material. This information had been of great value to infer in which direction the investigation described in this paper should point.

The main working principle of a phase change material states that it is capable of storing energy within its atomic chemical bonds as its phase change process occurs. The higher the latent heat of fusion value the greater will be the energy store capacity, without raising the material's temperature. These type of materials have been researched for decades and some are already commercially available to work together with specific construction materials. In the case

of concrete, special attention to the building structure integrity is necessary since as the PCM package passes through the melting process, the structural resistance of the material inside the container to either axial or shear stress is nearly zero (liquid phase). Therefore, the PCM layer has to be applied similarly to an insulation material layer, without compromising the structural resistance of the masonry and also allowing enough space for dilation as for most materials there is a small density variation between solid and liquid phases. The PCM needs to be engineered so that this density change is the smaller possible in order to avoid possible cracks along bricks, structural concrete or the concrete plaster.

The types of PCM that are able to be used as energy storage means are organic, eutectics and inorganic. A published work (Cabeza et al., 2011) describes all PCM types along with classification systematics, eventual problems and possible solutions when these materials are applied to buildings. Cabeza et al., (2011) also describes the chemical composition of many PCMs, including thermophysical properties as melting temperature, heat of fusion, thermal conductivity and density, which will certainly be useful to the development of the preliminary solution described in this abstract. Yaping et al., (2015) also describes the integration of PCMs in building walls for energy saving purposes, and correlates the type of PCM with the global regions it is more frequently used. Therefore, in order to contribute to the development of this research field the work presented in this article aims to map the thermal behavior of different PCMs vertically positioned along the concrete-brick structure by plotting average volume fraction and average temperature versus time as well as visually investigate the phase change progression in a small cross sectional area.

2. NUMERICAL MODEL

The heat transfer problem described in this paper can be solved by using a few numerical models that governs the multi physics involved in the solution. There are three main models that are directly evolved in the phase change layer of the material: the Eulerian Multiphase Model, which basically solves momentum, enthalpy and continuity equations for each phase of the material and tracks volume fractions (it also uses a single pressure field for all phases); the second model is the Reynolds Averaged Navier-Stokes, which is most commonly used due to its low cost in terms of compute power and run times; finally, the third model is the Volume of Fluid (VOF) which uses free surface approximation. This last model is described by a grid, which can be either stationary or non-stationary. More details about other models used in the solution of this case will be discussed as the work progresses.

2.1 Transport Equations

For the problem described in this abstract, as the melting occurs, the solid phase develops itself as an incompressible fluid, which will be subjected to natural convection due to variations in fluid density and gravity effects. As stated before, momentum, enthalpy and continuity equations are solved in the Eulerian Multiphase Model.

Momentum Equation for phase ‘k’ is given by:

$$\frac{\partial}{\partial t}\alpha_k \rho_k u_k + \nabla .\alpha_k \rho_k u_k u_k = -\alpha_k \nabla p + \alpha_k \rho_k g + \nabla \alpha_k \left(\tau_k + {\tau_k}^t\right) + M_k \tag{1}$$

where α is the volume fraction, ρ is the fluid density, u is the fluid velocity, p is pressure, g is gravity acceleration τ is shear stress, and M_k is the sum of interfacial forces.

Continuity equation:

$$\frac{\partial \rho}{\partial t} + \nabla .\left(\rho \vec{V}\right) = 0 \tag{2}$$

where V is the fluid velocity.

Furthermore, the conservation of mass and energy equations are also used in this model:

Conservation of mass for phase ‘k’:

$$\frac{\partial}{\partial t}\alpha_k \rho_k + \nabla .\alpha_k \rho_k u_k = \sum_{j=1}^{N}\left(\dot{m}_{jk} - \dot{m}_{jk}\right) \tag{3}$$

where N is the total number of phases and $\dot{m}$ is the mass transfer rate.

Conservation of energy for phase 'k':

$$\frac{\partial}{\partial t}\left(\alpha_k \rho_k h_k\right) + \nabla.\left(\alpha_k \rho_k u_k h_k\right) - \nabla\left[\alpha_k\left(\lambda_k \nabla T_k + \frac{\mu_t}{\sigma_h}\nabla h_k\right)\right] = Q_k \tag{4}$$

where λ is thermal conductivity, T is temperature and Q is interfacial heat transfer.
Furthermore, for a PCM in solid state, the temperature at the end of a time step is given by:

$$T_{final} = T_{initial} + \left(\frac{q_1 + q_2}{m_{PCM} * C_{P,solid}}\right) \tag{5}$$

where $T_{initial}$ is the initial temperature, T_{final} is the final temperature, q_1 and q_2 are the heat flux through the PCM, m_{PCM} is the mass and $C_{P,solid}$ is the solid specific heat at constant pressure.

$$T_{final} = T_{initial} + \left(\frac{q_1 + q_2}{m_{PCM} * C_{P,liquid}}\right) \tag{6}$$

where $C_{P,liquid}$ is the liquid specific heat at constant pressure.

2.2 Material Properties

For the solution presented in this article four types of PCM were analyzed. Cabeza et al. performs a detailed description of important material properties such as melting temperature, heat of fusion, thermal conductivity and density for many PCMs. Another publicized works (Khasanshin, T. S., Samuilov, V. S., Shchemelev, A.P., 2009; Tong W., Tong. A., 2015) also presents physical data for Polyglycol E600, Paraffin and n-Heptadecane which will be particularly useful because it complements Cabeza et al., (2011). with other relevant properties such as the specific heat. Table 1 presents the material properties used in the solution described in this numerical study.

Table 1. Physical properties of analyzed phase change materials.

PCM Physical Properties						
Material	**Density [kg/m³]**		**Thermal Conductivity [W/m.K]**	**Specific Heat [J/kg.K]**	**Melting Point [K]**	**Latent Heat of Fusion [kJ/kg]**
	Solid	Liquid	Liquid	Liquid	Solid to Liquid	Solid to Liquid
Polyglycol E600	1232	1126	0.1897	2135.27	295.15	127.0
Paraffin C13 – C24	900	760	0.21	2100	295.15	189.0
n-Heptadecane	760	760	0.21	2214	294.85	171.0
Paraffin C18	0.774	0.814	0.148	2140	295.65	243.5

2.3 PCM Wall Configuration, Geometry and Heat Generation

The schematic represented in Figure 1 illustrates the simplest and most energy effective (Panayiotou, G. P. et al., 2016) displacement for the PCM placed in a masonry wall in order to keep interior temperature at comfort level.

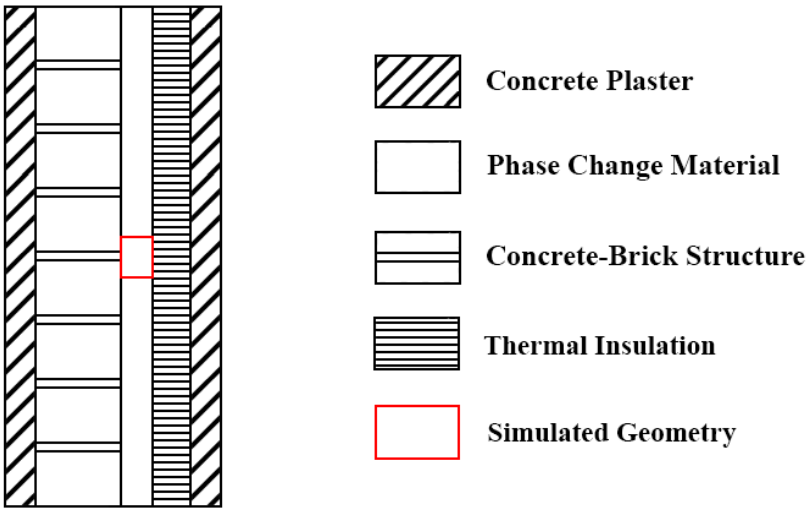

Figure 1. Simple masonry wall structure with integrated PCM.

The geometry used in the simulation consists in a simple rectangle vertically positioned (smaller edges horizontally displaced) with sides measuring 1 and 2 centimeters. This figure represents a small portion of the cross sectional area of the PCM and therefore it is purposely small enough to make it possible to visualize the phase change variation and also turn the simulation process into a less time consuming task. All common boundary conditions used in simulations are presented in Table 2.

Table 2. Simulation boundary conditions for all analyzed cases.

Simulation Boundary Conditions	
Left Wall	Solar Heat Flux
Right Wall	Adiabatic Wall
Top Wall	Symmetry Plane
Lower Wall	Symmetry Plane
Initial Temperature	295.0 K
Pressure	101325 Pa
Gravity	9.81 m/s²

Gueymard, C.A., (2003) describes that the solar radiation rate can reach peaks of 1366.1 W/m^2 at atmospheric level. In order to achieve a higher precision the heat flux incident to the vertical wall should be developed as a parabolic function of time. Olivieri, F. et al. estimates by experimental measures the solar radiation rate incident to a vertical wall and presents it as a line chart, which can be digitally read and converted to a two columns table in order to fulfill the needs of this study. Figure 2 presents the resultant solar heat flux (λ) [W/m^2] versus time [s] for a vertical wall.

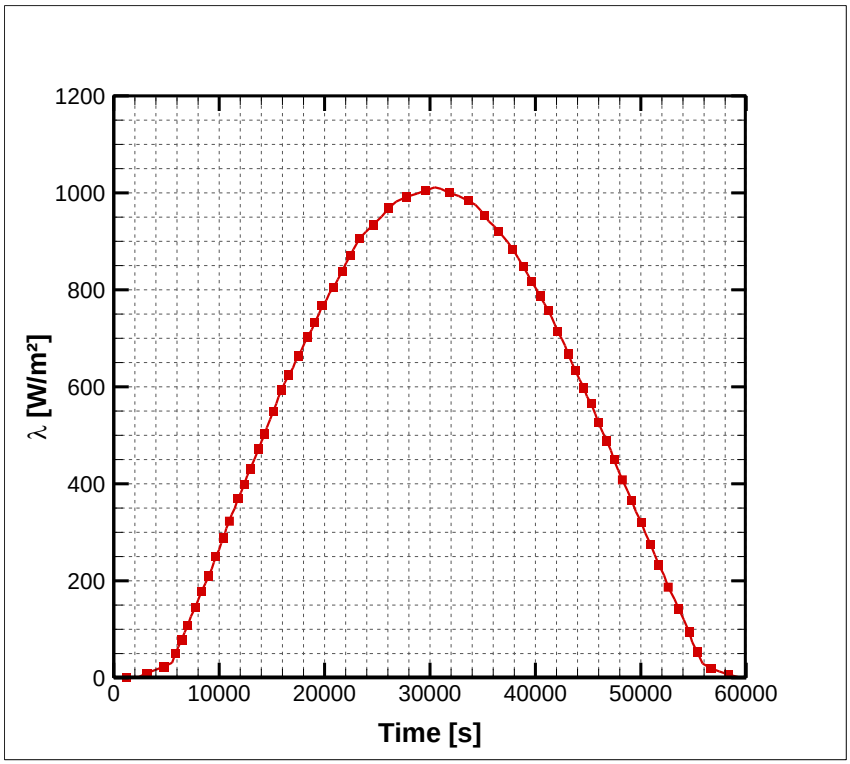

Figure 2. Solar heat flux (λ) [W/m^2] versus time [s] for a vertical wall.

Table 3 illustrates the main solver configurations used in all simulations performed.

Table 3. Solver configurations.

Solver Configurations	
Simulation Type	Implicit Unsteady
Time-Step	30.0
Maximum Physical Time	61000 s
Maximum Inner Iterations	40

2.4 Numerical Results

Numerical results were developed and compared for the problem described in this article. The time dependent heat flux boundary condition was applied to the left wall of the PCM container. Figure 3.a shows the first noticeable changes in the material's phase, after 20000 s of sunlight reception. This clearly happens because the PCM has a high heat of fusion, which characterizes it as a barrier for the trespassing heat. Figures b and c illustrates the progression of the phase change process in the PCM container (40000 and 60000 s).

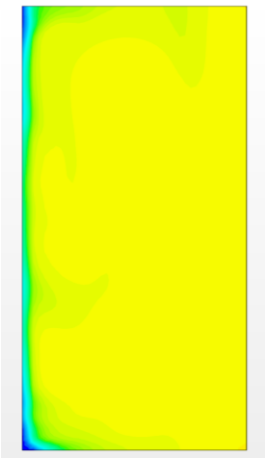

a) 20000 s.

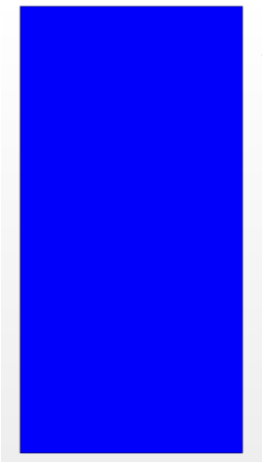

b) 40000 s.

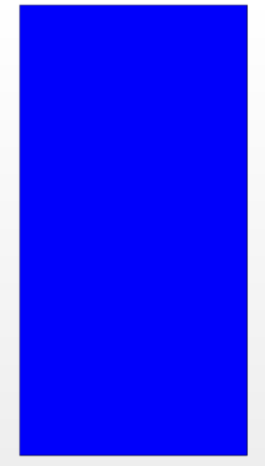

c) 60000 s.

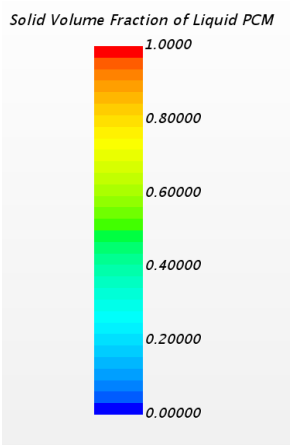

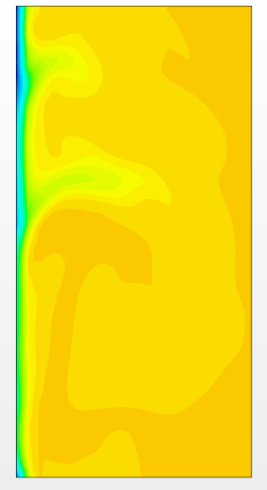

d) 20000 s.

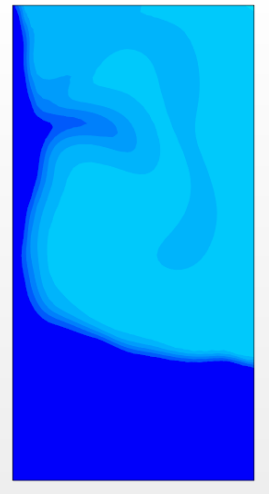

e) 40000 s.

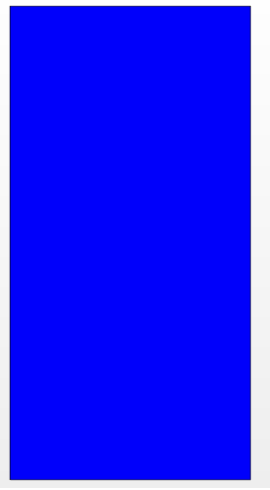

f) 60000 s.

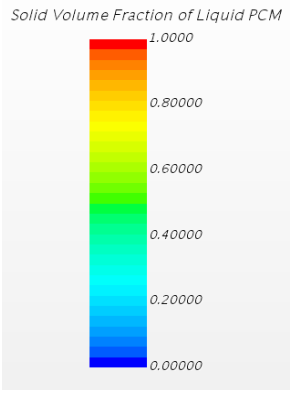

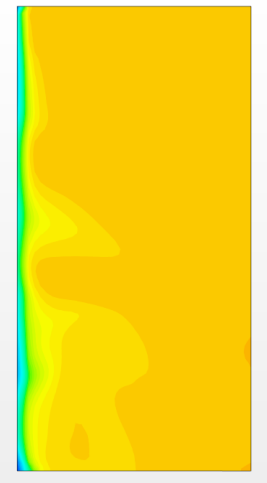

g) 20000 s.

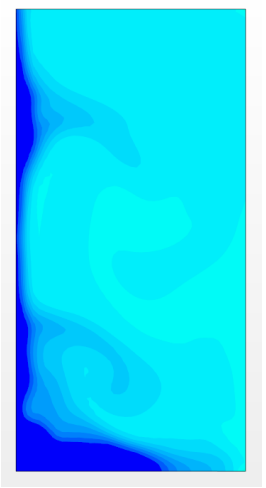

h) 40000 s.

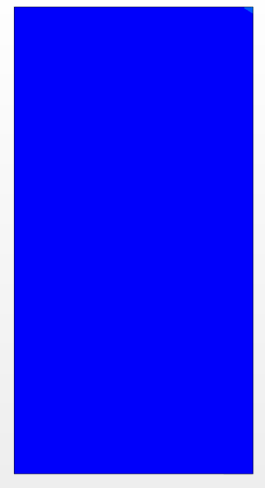

i) 60000 s.

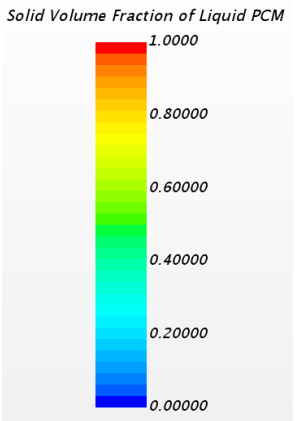

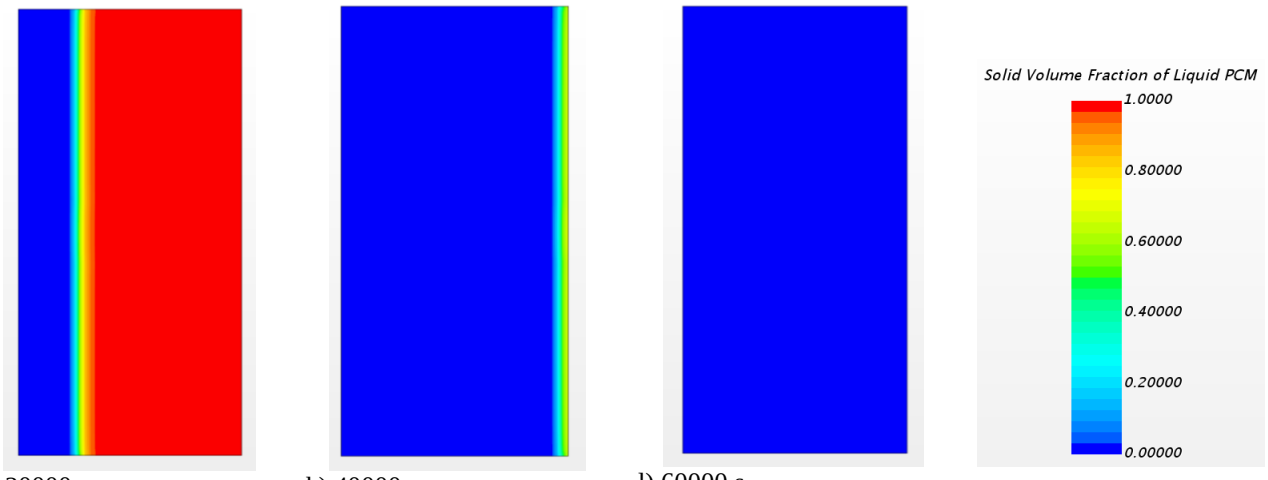

j) 20000 s. k) 40000 s. l) 60000 s.

Figure 3. Phase change progression (presented by solid volume fraction) as a function of time for 20000, 40000 and 60000 s: a, b, c) Polyglycol E600; d, e, f) n-Heptadecane; g, h, i) Paraffin $C_{13} - C_{24}$; j, k, l) Paraffin C_{18}.

The most efficient mean of comparing different phase change materials evolves investigating how much time is needed in order to complete the melting process when submitted to the same physical conditions. Therefore, analyzing the average solid volume fraction is of great help as it represents the progression of the phase change fronts alongside the computational domain. Figure 4 presents the average solid volume fraction (α) [W/m²] versus time [s] in the PCM container for all different materials analyzed in this article.

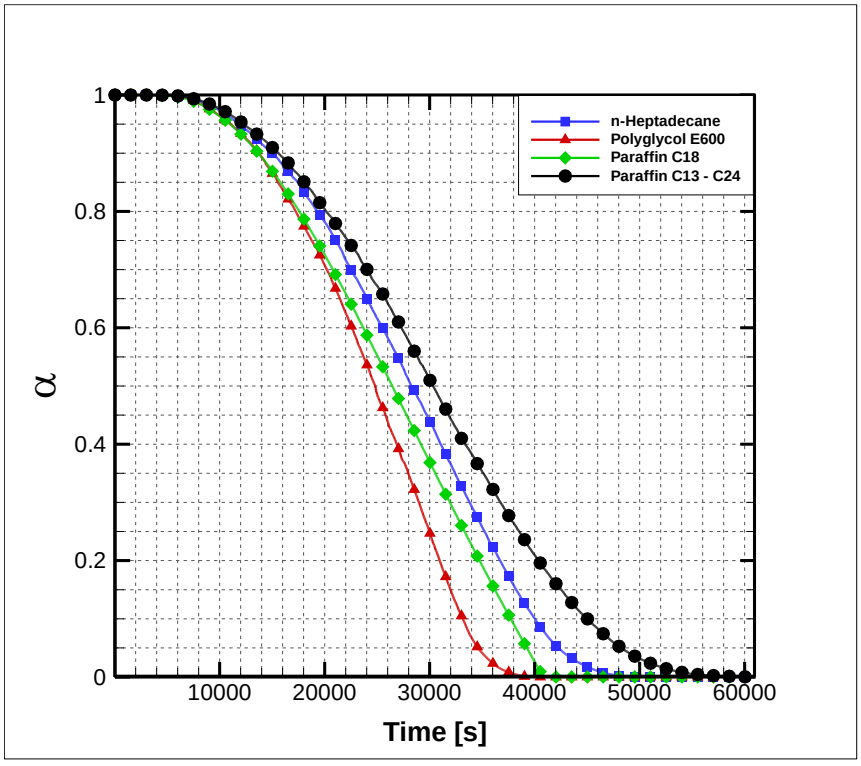

Figure 4. Average solid volume fraction (α) [W/m²] versus time [s].

As the study described in this article aims to compare the heat absorption efficiency for different materials, as important as analyzing the phase change progression is to investigate the domain average temperature behavior after melting process is complete. Figure 5 presents the average temperature (θ) [W/m²] versus time [s] in the PCM container.

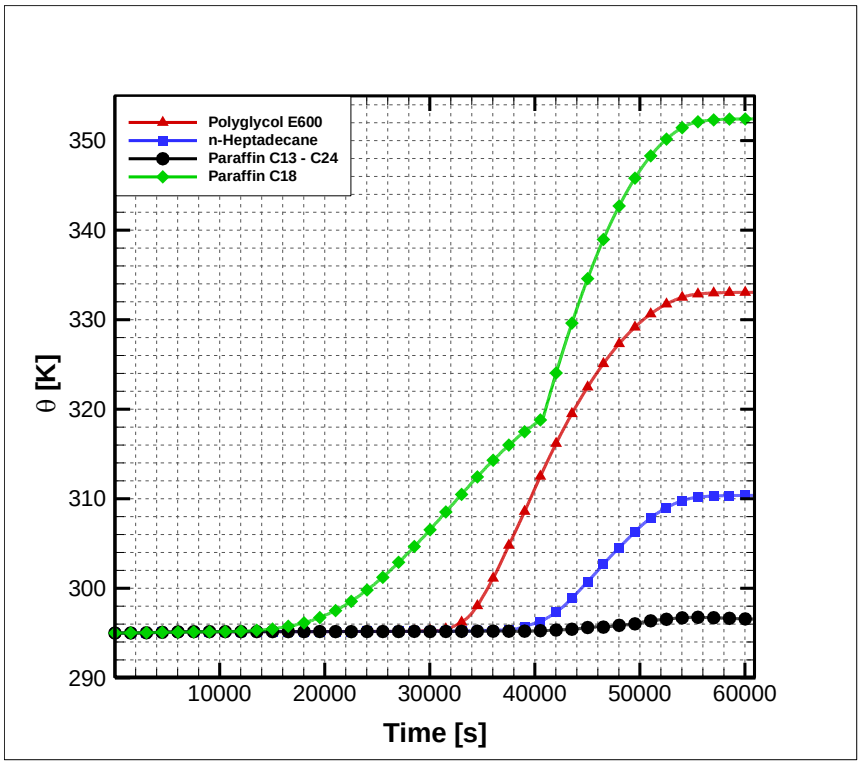

Figure 5. Average temperature (θ) [W/m^2] versus time [s].

2.5 Mesh Independency Study

The study presented in this article was performed using a triangular mesh generated by Star-CCM+ code. Figure 6 presents the solution conversion by analyzing the variation of the Average solid volume fraction (α) at 30000 s versus number of cells.

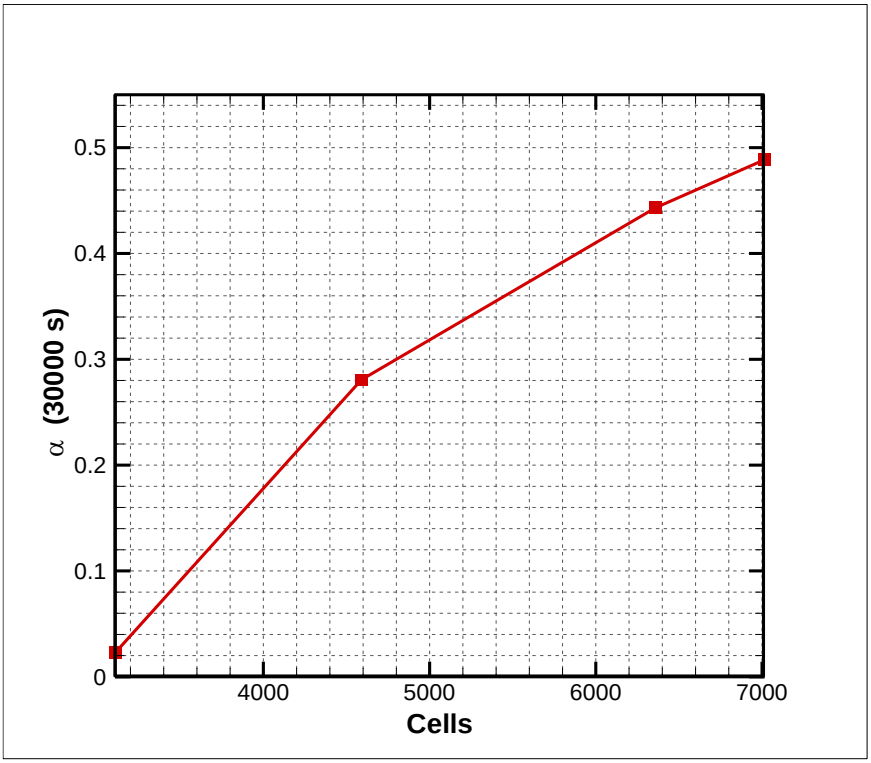

Figure 6. Average solid volume fraction (α) at 30000s versus number of cells.

The figure presented above illustrates the mesh conversion according to the number of nodes. As the number of cells increases, the average solid volume fraction tends to converge to a value close to 0.5. Analyzing the last stage of the chart (between 6360 and 7000 cells) it is possible to infer that the last 640 cells added to the mesh will only account for a variation of nearly 8.5 % in the results. Above 7000 s the simulation time will greatly increase and the change in the results will no longer be significant. As it was expected for a problem evolving a cavity phase change simulation the full convergence of the solution would demand an excessively large mesh. Therefore, for the solutions presented in this article, a mesh with 6360 cells was used, which perfectly balances simulation time and enough precision of the resultant data.

2.6 Conclusion

The numerical results presented are enough to conclude that Paraffin C13-C24 is the material with higher efficiency when it comes to maintain room temperature in comfort condition. Figure 5 clearly evidences that this material will hold the temperature to a lower value for a longer time. Figure 4 also evidences that Paraffin C13-C24 will take a longer time to complete the melting process. The results also state that even though Paraffin C18 is the material with the higher heat of fusion it is not the material with the best performance for the analyzed problem. This occurs due to its lower thermal conductivity, which eventually results the heat to be trapped in small portions of the material (evidenced in Figure 3. j, k, l)) in which the rise of temperature will modify physical properties sooner that if complete melting took longer to occur (it also facilitates paths alongside the material for trespassing heat). The results presented also concludes that n-Heptadecane will have a similar behavior to Paraffin C13-C24 for insolation times smaller than 40000 s, which can be particularly useful for walls or roofs where average insolation time is 12h or less, as a mean of cost savings.

3. ACKNOWLEDGEMENTS

The authors are thankful to SIEMENS PLM Software for their invaluable support with Star-CCM+ during this research. This study was financed in part by the Coordenação de Aperfeiçoamento de Pessoal de Nível Superior – Brasil (CAPES) – Finance Code 001.

4. REFERENCES

Cabeza, L.F., Castell, A. Barreneche, C., Gracia, A., Fernández, A.I., 2011. “Materials used as PCM in thermal energy storage in buildings”. *Renewable and Sustainable Energy Reviews*, Vol. 15, pp. 1675–1695.

Gueymard, C.A., 2003. “The sun’s total and spectral irradiance for solar energy applications and solar radiation models”. *Solar Energy*, Vol. 76, pp. 423 – 453.

Khasanshin, T. S., Samuilov, V. S., Shchemelev, A.P., 2009. “Determination of the thermodynamic properties of liquid n-hexadecane from the measurements of the velocity of sound”. *Journal of Engineering Physics and Thermodynamics*, Vol. 82, No. 1.

Olivieri, F., Grifoni, R. C., Redondas, D., Sánchez-Reséndiz, J. A., Tascini, S., 2017. “An experimental method to quatitatively analyse the effect of thermal insulation thickness on the summer performance of a vertical green wall”. *Energy and Buildings*, Vol. 150, pp. 132 – 148.

Panayiotou, G.P., Kalogirou, S.A. and Tassou S.A., 2016. “Evaluation of the application of Phase Change Materials (PCM) on the envelope of a typical dwelling in the Mediterranean region”. *Renewable Energy Journal*, Vol. 97, pp. 24–32.

Tong W., Tong. A., 2015. “Solar-absorbing metamaterial microencapsulation of phase change materials for thermo-regulating textiles”. *International Journal of Smart and Nano Materials*.

Yaping, C., Jingchao, X., Jiaping, L., Song, P., 2015. “Review of Phase Change Materials Integrated in Building Walls for Energy Saving”. *Procedia Engineering*, Vol. 121, pp. 763–770.

5. RESPONSIBILITY NOTICE

The authors are the only responsible for the printed material included in this paper.